REVISION 1

First evidence of $CaCO_3$-III and $CaCO_3$-IIIb - high-pressure polymorphs of calcite – authigenically formed in near surface sediments

Maike Schaebitz[1], Richard Wirth[2], Christoph Janssen[3], Georg Dresen[4]

[1] maike.schaebitz@gfz-potsdam.de ; +49 (0) 331/2881910
Helmholtz Centre Potsdam GFZ, German Research Centre for Geosciences,
Public Law Foundation State of Brandenburg, Telegrafenberg, 14473 Potsdam - Germany

[2] richard.wirth@gfz-potsdam.de ; +49 (0) 331/2881371
Helmholtz Centre Potsdam GFZ, German Research Centre for Geosciences,
Public Law Foundation State of Brandenburg, Telegrafenberg, 14473 Potsdam - Germany

[3] christoph.janssen@gfz-potsdam.de ; +49 (0) 331/2881323
Helmholtz Centre Potsdam GFZ, German Research Centre for Geosciences,
Public Law Foundation State of Brandenburg, Telegrafenberg, 14473 Potsdam - Germany

[4] georg.dresen@gfz-potsdam.de ; +49 (0) 331/2881320
Helmholtz Centre Potsdam GFZ, German Research Centre for Geosciences,
Public Law Foundation State of Brandenburg, Telegrafenberg, 14473 Potsdam - Germany

Abstract

Calcite is one of the most ubiquitous minerals in the earth's crust and is mostly present as calcite or the slightly denser polymorph aragonite. In addition five different phases of $CaCO_3$ (calcite II- VI), which display similar structural features as calcite, have been observed with increasing pressure in different experiments by several authors. Experimentally, the $CaCO_3$-III and $CaCO_3$-IIIb polymorphs have recently been observed by Merlini et al (2012) applying pressures between 2.5 - 15 GPa on natural samples of calcite using single - crystal synchrotron X-ray diffraction.

Here we report an occurrence of metastable authigenic $CaCO_3$-III and $CaCO_3$-IIIb nanocrystals for the first time in nature. Using Transmission Electron microscopy,

Always consult and cite the final, published document. See http://www.minsocam.org or GeoscienceWorld

idiomorphic, 50- 150 nm sized crystals were observed within several meters from the surface in quaternary loess deposits in Central Asia.

Nanocrystals contain higher surface energy per volume compared to coarse grained materials due to their larger surface area. The internal pressure of a solid P_S is at equilibrium with the surface stress, which increases with decreasing particle size. We estimated internal pressures inside the observed nanocrystals between 2.54 – 4.06 GPa, assuming spherical crystals with 1nm diameter and specific surface energies, between 1,27- 2,03 J/m^2 (Forbes et al., 2011).

Introduction

Calcium carbonate displays three polymorphs, aragonite (orthorhombic), vaterite (hexagonal) and calcite (trigonal), which is the most stable at ambient conditions. Vaterite and aragonite are metastable polymorphs that transform to calcite at ambient conditions. Their occurrence depends on small changes in temperature or pH (Han et al., 2006) during precipitation. Since the first discovery of high pressure modifications of calcite that differ from aragonite structure (calcite II and III) by Bridgman (1938) applying volumetric measurements, calcite III has been repeatedly produced experimentally. However, none of these polymorphs, except calcite-I, aragonite and vaterite, have been quenched and observed under ambient conditions (Biellmann 1993). Recently, Merlini et al. (2012) refined the unit cell data for $CaCO_3$-III (Cc-III) (triclinic) and introduced a triclinic structure named $CaCO_3$-IIIb (Cc-IIIb). Cc - IIIb is observed to form at similar pressures of 2.5- 15 GPa as Cc-III, however only if pressure is increased slowly avoiding significant overpressure. The Cc- IIIb polymorph is pseudo-monoclinic and has a lower density. The number of formula units per unit cell is 4 in Cc-IIIb as opposed to 10 in Cc-III. (Fig. 1, Table 1), (Merlini et al., 2014).

Always consult and cite the final, published document. See http://www.minsocam.org or GeoscienceWorld

Because of its higher energy content, Cc-IIIb is thermodynamically metastable with respect to Cc-III. In addition to calcite, five other modifications of $CaCO_3$, with basic structural features of calcite have been observed over a broad range of temperature and pressures (Fig 2).

We used Transmission Electron Microscopy (TEM) to investigate the microstructures of sliding surfaces of landslides in Kyrgyzstan and China, Central Asia and found nanocrystalline calcite in gouge material that interestingly could neither be identified as calcite, aragonite nor vaterite. Instead authigenic nanocrystals of the metastable high pressure calcite polymorph $CaCO_3$-III and $CaCO_3$-IIIb have been found for the first time in nature.

Geological setting/Study Area

In Kyrgyzstan samples have been taken from the first scarp sliding surface of a landslide located in quaternary loess (Fig. 3). The landslide extends over 0.1 km^2 and has an approximate volume of 400.000 m^3. The sample location is situated 40 km southeast of Osch in the Fergana basin close to a roadside at the M 41. Loess deposits up to 50m thick cover large areas in the foothills of the Fergana basin in SW Kyrgyzstan (Roessner et al., 2005). The mineralogy of the deformed loess samples is dominated by fine grained quartz, some feldspar, sheet silicates (mainly illite) and carbonates.

We also sampled a landslide 20 km north- east of Longnan (Province of Gansu) in Central China. The sliding surface of the landslide is well exposed and up to 20 cm thick. It forms the base of up to 5m thick quaternary loess deposits covering silurian phyllite. The $CaCO_3$ high pressure polymorphs were found in the transition area of the sliding surface to the overlying loess deposits. The two sample locations in Kyrgyzstan and Gansu display similar climate conditions. Both regions are tectonically active and characterized by large loess deposits that are often affected by destructive mass movements related to snow melting, heavy rainfalls

Always consult and cite the final, published document. See http://www.minsocam.org or GeoscienceWorld

and/or earthquakes. The climate in SW Kyrgyzstan and Gansu is continental, but the Gansu is partly affected by monsoon rains.

Sample preparation and methods

To conserve the original, undisturbed structure of the sliding surface and about 20 cm of sediment below, we took the samples using 8 cm diameter and 20 cm long metal tubes. The sample tubes were pushed carefully into the soil approximately normal to the sliding surface using a hammer and plastic extension on top of the tubes. In order to prevent drying or moving of the contents, the tubes were wrapped in think layers of plastic film. For the preparation of thin sections the metal tubes were cut open into two equal parts, parallel to the long axis. To not affect the mineral content and microstructure by swelling of clay minerals, samples were polished dry.

Samples for thin sections were taken from directly the sliding surfaces itself (see Fig. 4) and at increasing distances to the surfaces. For thin section preparation the samples were embedded in epoxy to stabilize the material. After evaluating the characteristics of the microstructure in a sample using a transmitted light microscope, the area for the TEM investigations was marked on high resolution optical scans of the thin section. At GeoForschungsZentrum (GFZ) Potsdam these samples are prepared for transmission electron microscopy (TEM) in routine using a focused ion beam (FIB) device (FEI FIB200TEM) that avoids preparation induced damage (Wirth 2004, 2009). The microstructures were analyzed in TEM using a FEI Tecnai G2 F20 X-Twin transmission electron microscope (TEM/AEM) at GFZ Potsdam. The small size of the Cc nanocrystals and their sensitivity to electronic radiation damage did not allow the acquisition of convergent electron diffraction patterns. To overcome the problem of electron irradiation damage, diffraction patterns were calculated from high-resolution lattice fringe images by Fourier transforms (FFT). The acquisition time

Always consult and cite the final, published document. See http://www.minsocam.org or GeoscienceWorld

for acquiring a high-resolution image on the CCD camera was 0.7 seconds. High-angle annular dark-field imaging (HAADF) was performed with two different camera lengths. The scattering intensity and the scattering angle of an atom depends on its atomic number (Z). Selecting an appropriate camera length allows imaging different contrasts. Short camera length (75 mm) collects the electrons that are scattered under a high-angle resulting in Z-contrast only. Increasing the camera length (330 mm) allows to acquire images with diffraction contrast plus Z-contrast.

TEM observations

We investigated samples taken from the sliding surfaces and the host rock surrounding. The TEM overview image of a sample from Kyrgyzstan shows calcite and quartz grains surrounded by a layered mixture of clay minerals (Mg-Al-Si) and chlorite. Authigenic $CaCO_3$-IIIb is growing into the pore space across the entire sample (Fig. 5). The second TEM overview image (Fig. 6) represents a sample from Gansu, China. Partly weathered sheetsilicates are surrounded by a mixture of newly formed $CaCO_3$-III, $CaCO_3$-IIIb and new sheetsilicates. The Cc-III and Cc-IIIb crystals typically occur in open pore space (Fig. 5,6,7). There is no evidence from (micro-) structures or mineral content for a high pressure deformation event.

The idiomorphic carbonate crystals are nanocrystalline with an average grain size of 70 nm (Fig. 7) and show approximately the same size in all samples. The crystals are elongated (Fig. 7) and show diffraction contrasts (see marked example in Fig. 7). Most crystals (Fig. 7) display non equate cross – sections suggesting a shape – preferred orientation.

Electron diffraction X-ray (EDX) spectra did confirm that the composition of single crystals for further analysis at high-resolution was a $CaCO_3$ phase (Fig. 8). Calculated diffraction patterns from high-resolution lattice fringe images (fast Fourier Transforms FFT) were used

Always consult and cite the final, published document. See http://www.minsocam.org or GeoscienceWorld

to identify the carbonate phase as Cc- III (Fig. 9) and Cc-IIIb (Fig. 10). The diffraction patterns could be completely indexed as Cc-III and Cc-IIIb, respectively. We measured the lengths of the diffraction vectors from the FFT images and converted them into lattice plane d-spacing. Additionally, the angles between the diffraction vectors were measured from the diffraction patterns. The observed d-spacings and the angles between adjacent lattice planes were compared with calculated data based on the crystal structure of Cc-III and Cc-IIIb, calcite and aragonite. The observed data did not fit the calculated data of aragonite, calcite or vaterite. However, we found a very good agreement between calculated and observed crystal lattice data for the calcite phases Cc-III and Cc-IIIb (Table 1).

Discussion

The occurrence of nanometer-sized crystals of high P- (T) polymorphs in rocks has been discovered before. Here we demonstrate for the first time that these nanocrystals of high P phases form at ambient conditions in aeolien sediments just a few meters below the surface.

Biellmann (1993) quenched and oberseved calcite II from moderately heated calcite pressurized at 45 GPa, but none of the high pressure polymorphs of calcite –except aragonite- have been observed to form at ambient conditions. For our samples we can exclude any indications for a high pressure or high stress dynamic impact related to the landslide activity on the samples. However creeping or episodic slip of the landslide may cause comminution and control microstructure such as Cc-III and Cc-IIIb nanocrystals.

Bridgman (1939) suggested that under geological conditions, temperatures in the crust are to high at the prevailing pressures to allow for a (macro)phase transition of Cc-II to Cc-III. However, stability conditions for nanocrystalline materials, are expected to be very different from those of macroscopic materials due to their extremely small particle size. The formation of metastable high pressure phases is well known. For example in the early 1950's it became

Always consult and cite the final, published document. See http://www.minsocam.org or GeoscienceWorld

possible to synthesize diamond at low pressures and moderate to high temperatures and even in ultrahigh vacuum by chemical vapor deposition (Discher et al., 1998). Nanometer-sized diamonds are also common in primitive chondrites (Kennet et al., 2009) and have been found in melt inclusions in Hawaiian lavas (Wirth & Rocholl, 2003).

Banfield and Zhang (2001) suggest that nanocrystals structures and properties are different than those of macroscopic crystals, dominated by a periodic structure. In contrast, with decreasing particle size surface effects become important. In contrast to the periodic structure of the crystals interior, the surface structure of a crystal is severely distorted because it consists of ions with their electronic charges being unbalanced due to interrupted coordination sites. As a result the surface carries excess energy, the surface free energy (γ). In order to minimize the total energy of the system, surface atoms try to rearrange, causing a set of relative displacements resulting in a surface strain and a corresponding surface stress *(f)*.

The existence of the Cc-III and Cc-IIIb polymorphs in nano-particles, commonly stable in the pressure range of 2.5 – 15 GPa (Merlini, Hanfland et al., 2012), suggest that elevated surface tension in equilibrium with internal pressure may affect phase stabilities of nanosized crystals (Banfield and Zhang, 2001). For most solids, f is generally of the same order of magnitude as γ, being equal or up to 3 times greater (Cammarata & Sieradski, 1994). A tensile surface stress, shrinking the unit cell parameters, is present in case f is positive (Banfield and Zhang 2011). From calorimetric data, the surface energies of calcite were determined to be 1.48 ± 0.21 and 1.87 ± 0.16 J/m^2 for hydrous and anhydrous surfaces (Forbes et al., 2011).

Assuming $f \geq \gamma$, the pressure acting on a spherical particle with radius r is:

$$P = \frac{4\,\gamma\,(J/m^2)}{D\,(nm)}\,GPa \qquad (1)$$

Always consult and cite the final, published document. See http://www.minsocam.org or GeoscienceWorld

P is the pressure (Pa), γ is the surface free energy = surface stress or tension (J/m^2), r the radius and D the diameter (nm) of a spherical particle.

The pressure P required for the formation of $CaCO_3$-III(b) may exist in particles with grain sizes up to 2 nm (Fig. 11). However TEM images show calcite grainsizes in our samples between 50- 150 nm. We suggest that particles precipitated rapidly from an aqueous solution at low temperatures when diffusion and/or recrystallization are slow. Then the initial structure, controlled by the initial precipitation conditions may persist metastable (Navrotsky, 2011). This assumes that during precipitation and nucleation of the crystal, pressures were sufficiently high to allow Cc-III and Cc-IIIb formation. We speculate that particles formed by oriented cluster attachment growth (Fig. 8) (Banfield and Zhang, 2001). The formation of nanoclusters is crystallographically controlled and cluster attachment minimizes surface energy of the system.

Implications

It has been known from experiments for nearly a century that the very common mineral calcite undergoes serveral phase transitions with increasing pressure, but some of the described polymorphs have never been observed before in nature.

Analyzing microstructures of sliding surfaces from landslides using TEM and the focused ion beam (FIB) technique, we found authigenic nanometer-sized crystals of two high pressure polymorphs of calcite, $CaCO_3$-III and $CaCO_3$-IIIb that clearly formed close to the Earth's surface at almost ambient pressure. The observed crystal structures have up to now only been found experimentally at high pressure (Merlini et al,. 2014).

We found both structures initially described by Merlini et al (2012) within on sample, confirming the possible coexistence as nanoparticles formed at ambient conditions in nature.

As calcite plays an important role in the global geochemical cycles of C its stability and possible high pressure structures in the Earth's mantle are a matter of an ongoing debate

Always consult and cite the final, published document. See http://www.minsocam.org or GeoscienceWorld

(Merlini et al., 2012; Biellmann et al., 1993) and amongst others $CaCO_3$-III and $CaCO_3$-IIIb are discussed as possible host structures, but the conditions on which they get adopted by carbonates in nature had to be established and we can show the first example.

Our findings confirm that experimental results and assumptions from several authors, which demonstrate that high surface stresses may generate high pressure phase nanoparticles outside their stability field (Banfield and Zhang, 2001), does also occur in nature. Also finding these two polymorphs in two different samples at different geological settings several thousands of kilometers apart supports our conclusion that the formation of high pressure polymorphs on the nanoscale due to high surface stresses may be more common in geological materials than expected.

Acknowledgments

We thank Artem R. Oganov and an anonymous reviewer for giving useful comments and suggestions. We are grateful to Prof. Xingmin Meng from Lanzhou University for arranging the field campaign in China and Dr. Hans-Ulrich Wetzel and Dr. Sigrid Roessner for guiding us in the field in Kyrgyzstan. We also would like to thank Anja Schreiber for TEM foil preparation using FIB technique, and Stefan Gehrmann for the preparation of thin sections.

This work is financially supported by the Bundesministerium für Bildung und Forschung (BMBF).

Always consult and cite the final, published document. See http://www.minsocam.org or GeoscienceWorld

231

232 **Figure captions**

233

234 Fig. 1: Phase relations of $CaCO_3$ polymorphs, experimental data. Bold lines: modified after
235 Suito et al., 2001, dashed lines: after Merlini et al., 2012.

236

237 Fig. 2: Crystal structures of a) triclinic $CaCO_3$-III and b) triclinic $CaCO_3$-IIIb after Merlini et
238 al., 2012. Red spheres: oxygen, black carbon, blue calcium atoms. The blue frames mark the
239 unit cell, indicating Cc-III (10 units per unit cell) has a larger density than Cc-IIIb (4 units per
240 unit cell). Y points to the crystallographical b- axis.

241

242 Fig. 3: a: The white circle marks the sampling area at the headscarp of a landslide located in
243 quaternary loess in Kyrgyzstan.

244

245 Fig. 4: Landslide sample with sliding surface, which is retraced as a white dotted line on the
246 left side. The white box marks the area of the thinsection that is showen as inset. Positions of
247 the FIB foils for TEM analysis are marked. The macrostructure in the thin section shows no
248 features pointing to movement; the positions for FIB are random. The change in color from
249 darker to bright orange is due to oxidized ironoxid.

250

251 Fig. 5: High-angle annular dark field image: Part of an overview image of a FIB foil showing
252 the characteristic locations of $CaCO_3$-IIIb crystals in all our samples: surrounded by
253 sheetsilicate in open pore space. Examples of Calcite IIIb crystals are marked inside the three
254 white rings. The sample was located in southwestern Kyrgyzstan.

255

Always consult and cite the final, published document. See http://www.minsocam.org or GeoscienceWorld

Fig. 6: HAADF picture: Part of an overview image of a FIB foil also showing $CaCO_3$-IIIb and $CaCO_3$-III crystals (white arrows) surrounded by sheetsilicate in open pore space, indicating the absence of a high-pressure regime. Examples of $CaCO_3$-IIIb and $CaCO_3$-III crystals are marked with white arrows. The sample was located in central China.

Fig. 7: TEM bright field image showing the elongated morphology and local diffraction contrast of the $CaCO_3$-IIIb crystals and their characteristic frequent occurrence in open pore space. In many crystals local dark diffraction contrast along their long axis is visible, which is maybe due to local dislocations in the crystal lattice that developed while oriented attachment growth or twinning.

Fig. 8. Energy dispersive X-ray intensity spectrum of the $CaCO_3$-III nanocrystal in figure 8. Gallium scattering intensity is due to implanted Ga-ions during FIB sample preparation. The copper peak is caused by X-Ray photons from the copper grid. The unusual high carbon concentration is caused by the Epoxy.

Fig. 9. High-resolution electron microscopy image of a single $CaCO_3$-III crystal with zone axis [0-2-1] with the corresponding diffraction pattern in the upper right corner. In the lower right corner a second crystal can be seen which is connected to the central one in nearly the same crystallographic orientation.

Fig. 10. High-resolution electron microscopy image of a single $CaCO_3$-IIIb crystal with zone axis [120]. The inserted diffraction pattern contains additional reflections from at least two other crystals, one in the upper right corner (partially covered by the diffraction pattern) and the other crystal in the lower right corner. Some amorphous material between two crystals is marked within the white line.

Always consult and cite the final, published document. See http://www.minsocam.org or GeoscienceWorld

Fig. 11. Principle calculations of surface pressure P against grain diameter (assuming spherical particles) for the lowest surface energies of calcite, 1,27 J/m^2.

Tables

Table 1 Measured d-spacing and the angles between adjacent planes of Cc- III, Cc-IIIb in comparison to the data of Merlini et al., 2012 and to aragonite and calcite.

References

Banfield, J.F., and Zhang, H. (2001) Nanoparticles in the Environment. Reviews in Mineralogy and Geochemistry, 44(1), 1-58.

Biellmann, C., Guyot, F., Gillet, P., and Reynard, B. (1993) High-pressure stability of carbonates: quenching of calcite-II, high-pressure polymorph of CaCO3. European journal of mineralogy, 5(3), 503-510.

Biellmann, C., Gillet, P., Guyot, F.o., Peyronneau, J., and Reynard, B. (1993) Experimental evidence for carbonate stability in the Earth's lower mantle. Earth and Planetary Science Letters, 118(1–4), 31-41.

Bridgman, P.W. (1938) The high pressure behavior of miscellaneous minerals. American Journal of Science, 237(1), 7-18.

Cammarata, R.C., and Sieradzki, K. (1994) Surface and interface stresses. Annual Review of Materials Science, 24(1), 215-234.

Dischler, B., and Wild, C. (1998) Low-pressure synthetic diamond: manufacturing and applications. Springer Heidelberg.

Forbes, T.Z., Radha, A.V., and Navrotsky, A. (2011) The energetics of nanophase calcite. Geochimica et Cosmochimica Acta, 75(24), 7893-7905.

Merlini, M., Crichton, W., Chantel, J., Guignard, J., and Poli, S. (2014) Evidence of interspersed co-existing CaCO3-III and CaCO3-IIIb structures in polycrystalline CaCO3 at high pressure.

Always consult and cite the final, published document. See http://www.minsocam.org or GeoscienceWorld

Mineralogical Magazine, 78(2), 225-233.

Merlini, M., Hanfland, M., and Crichton, W.A. (2012) CaCO3-III and CaCO3-VI, high-pressure polymorphs of calcite: Possible host structures for carbon in the Earth's mantle. Earth and Planetary Science Letters, 333–334(0), 265-271.

Navrotsky, A. (2011) Nanoscale effects on thermodynamics and phase equilibria in oxide systems. ChemPhysChem, 12(12), 2207-2215.

Roessner, S., Wetzel, H.-U., Kaufmann, H., and Sarnagoev, A. (2005) Potential of satellite remote sensing and GIS for landslide hazard assessment in Southern Kyrgyzstan (Central Asia). Natural Hazards, 35(3), 395-416.

Wirth, R. (2004) Focused Ion Beam (FIB) A novel technology for advanced application of micro-and nanoanalysis in geosciences and applied mineralogy. European Journal of Mineralogy, 16(6), 863-876.

-. (2009) Focused Ion Beam (FIB) combined with SEM and TEM: Advanced analytical tools for studies of chemical composition, microstructure and crystal structure in geomaterials on a nanometre scale. Chemical Geology, 261(3), 217-229.

Always consult and cite the final, published document. See http://www.minsocam.org or GeoscienceWorld

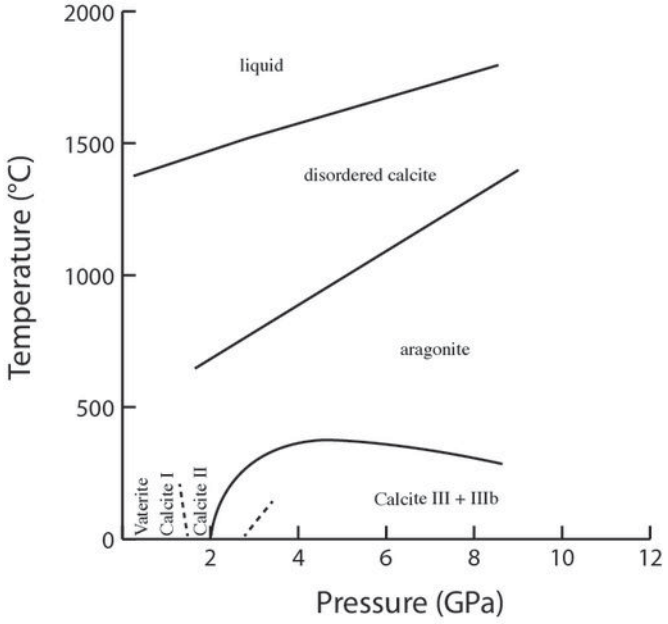
2000
1500
1000
500
0
Temperature (°C)
liquid
disordered calcite
aragonite
Vaterite
Calcite I
Calcite II
Calcite III + IIIb
2
4
6
8
10
12
Pressure (GPa)

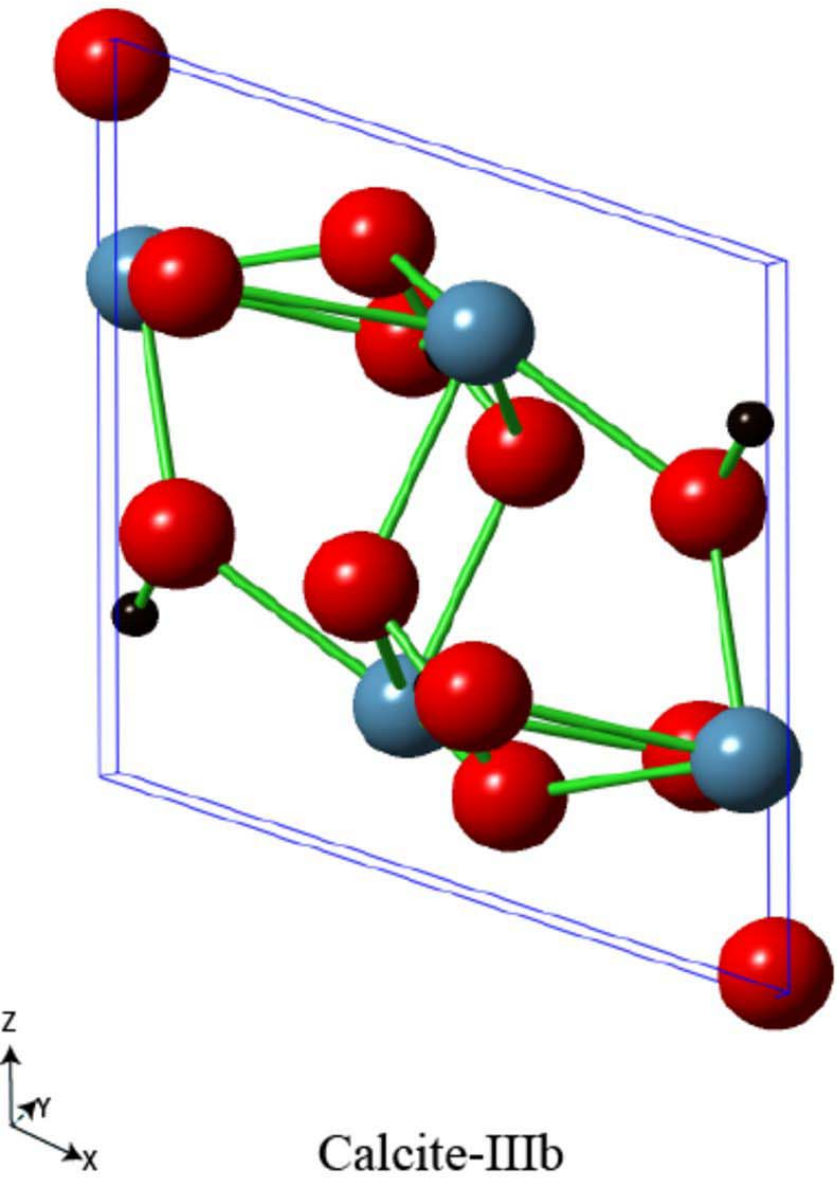

Calcite-IIIb

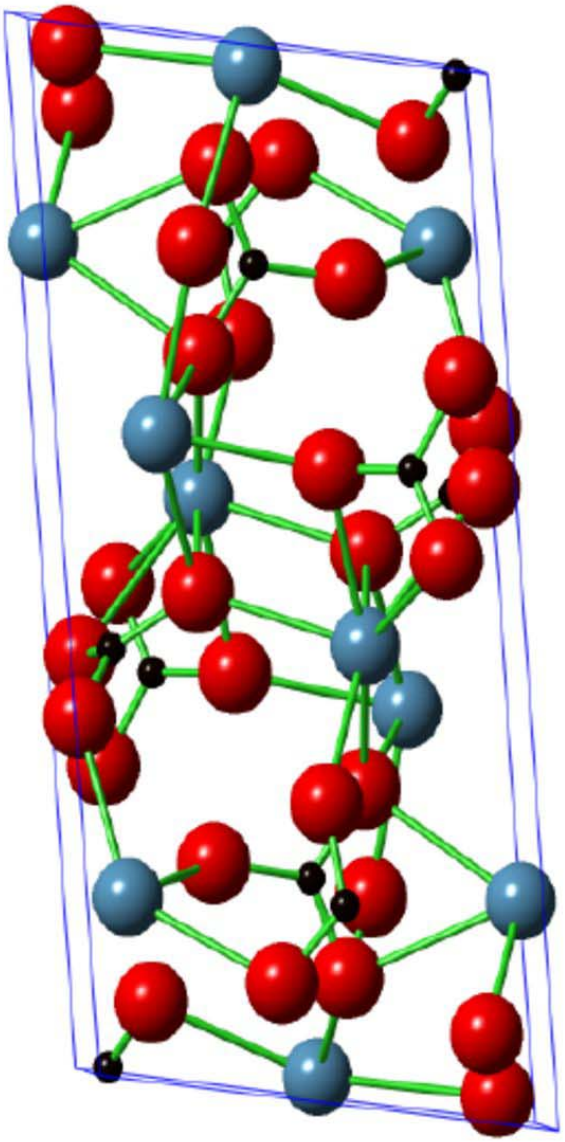

Calcite-III


Sampling Area
50cm

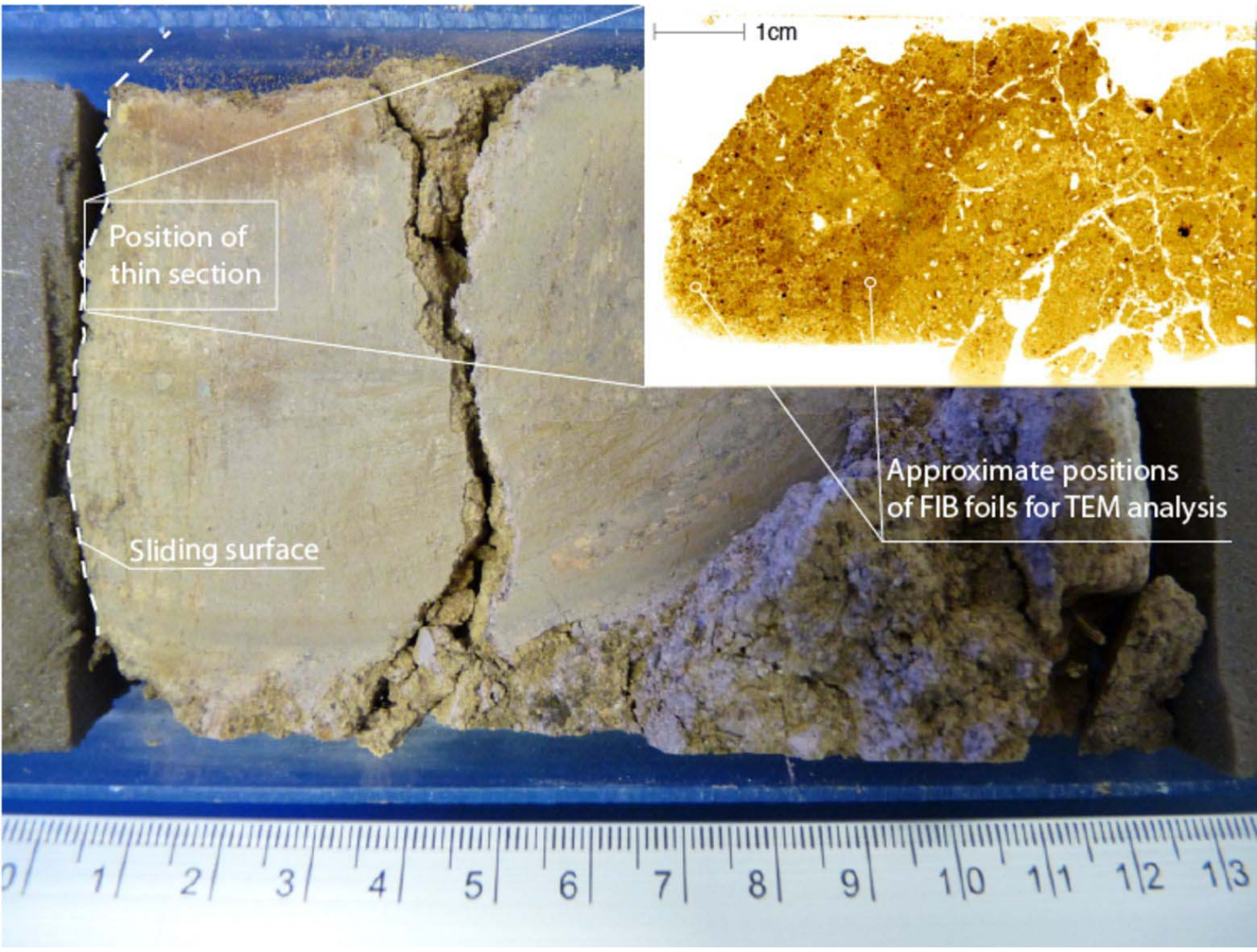
1cm
Position of thin section
Approximate positions of FIB foils for TEM analysis
Sliding surface

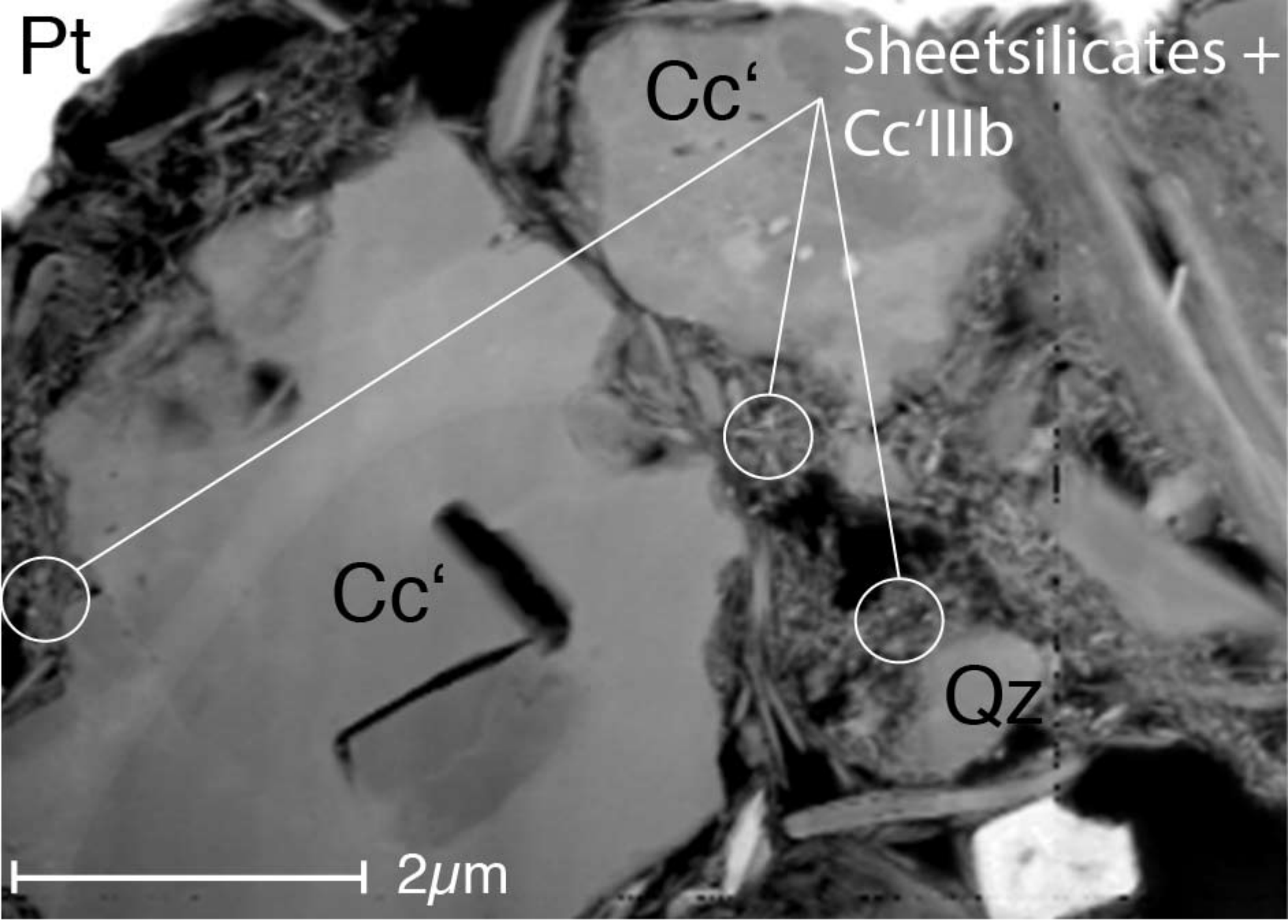
Pt
Cc‘
Sheetsilicates +
Cc‘IIIb
Cc‘
Qz
2μm


Sheetsilicates
500nm

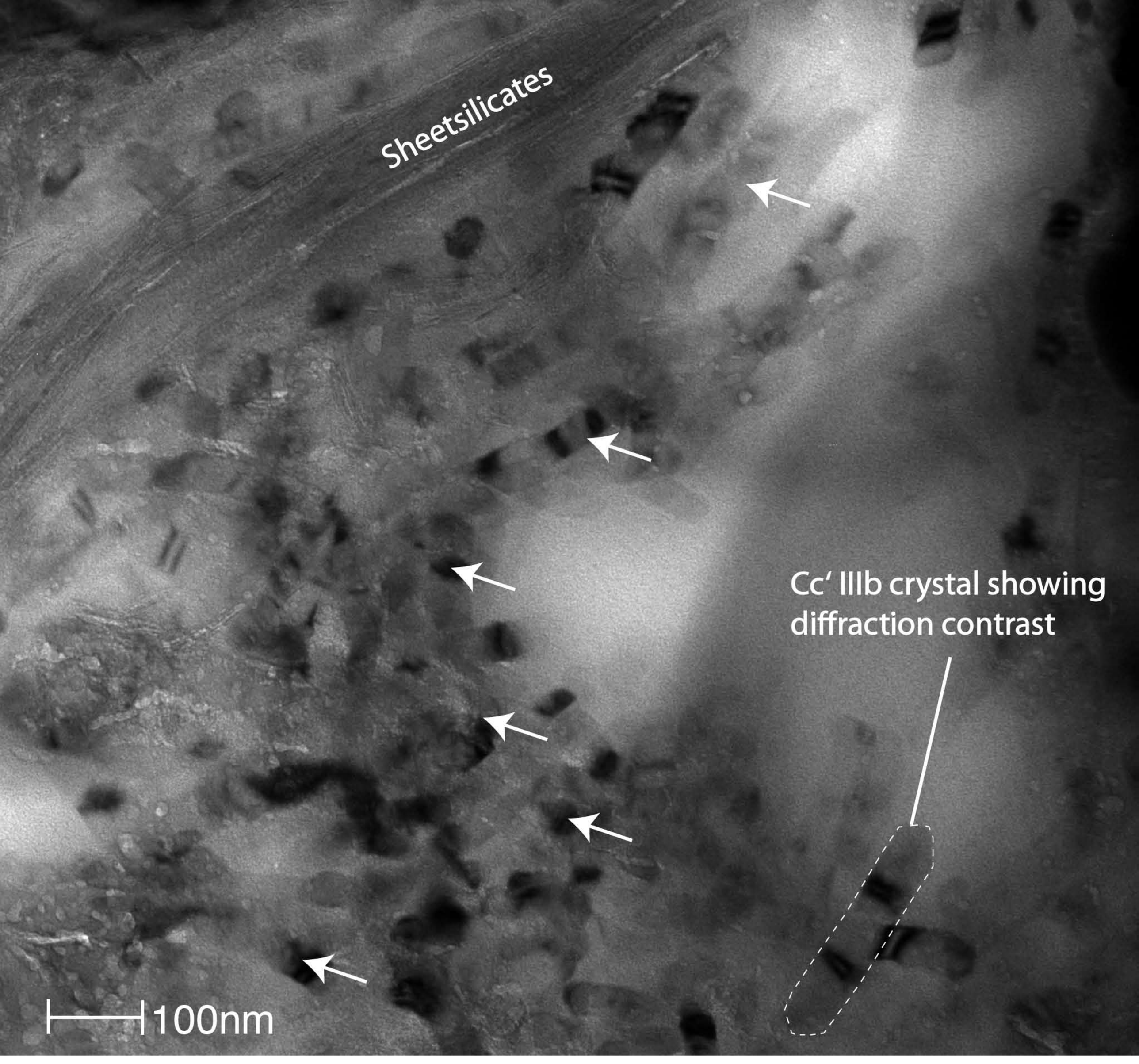
Sheetsilicates
Cc‘ IIIb crystal showing diffraction contrast
100nm

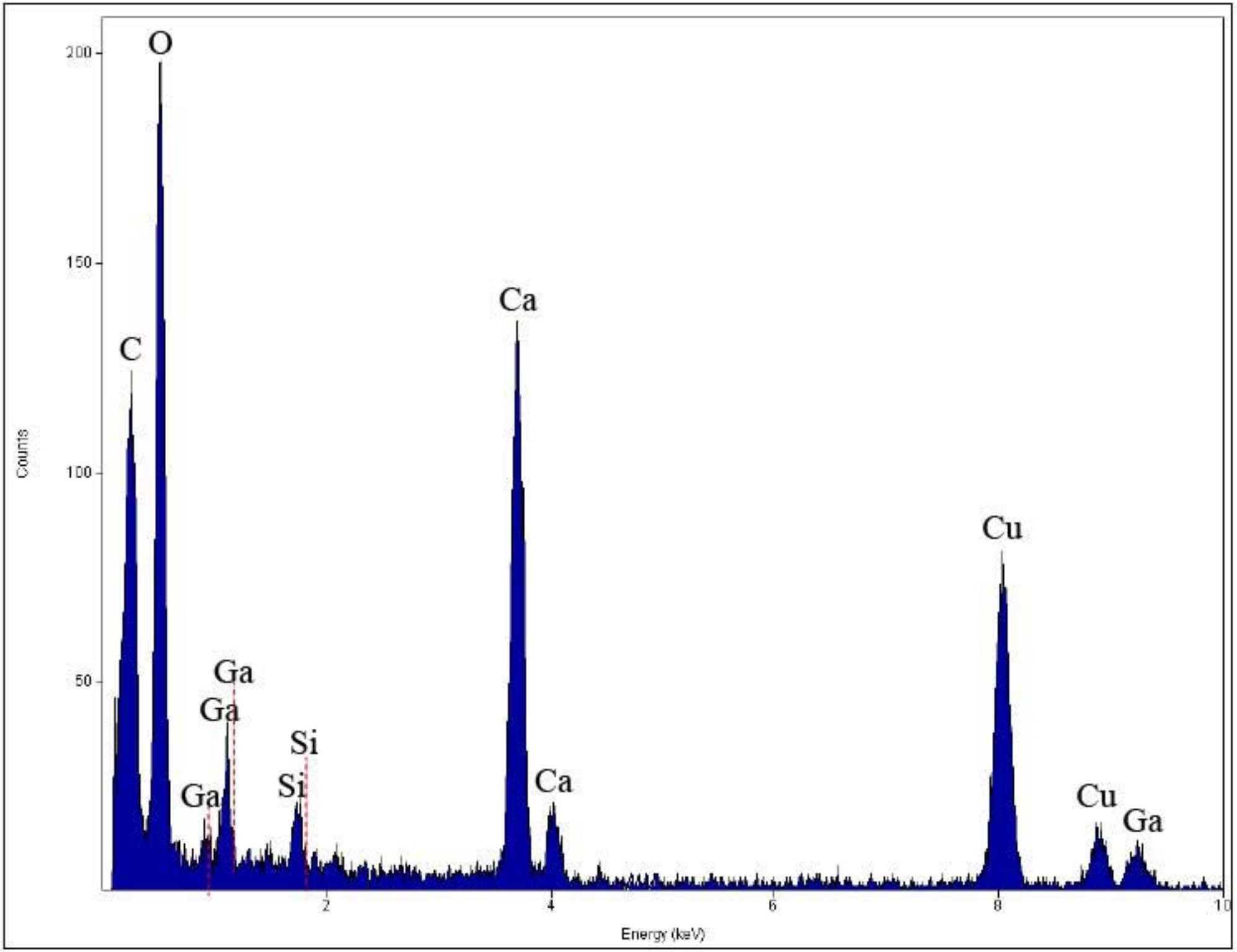
O
C
Ca
Cu
Ga
Ga
Ga
Si
Si
Ca
Cu
Ga
200
150
100
50
Counts
2
4
6
8
10
Energy (keV)

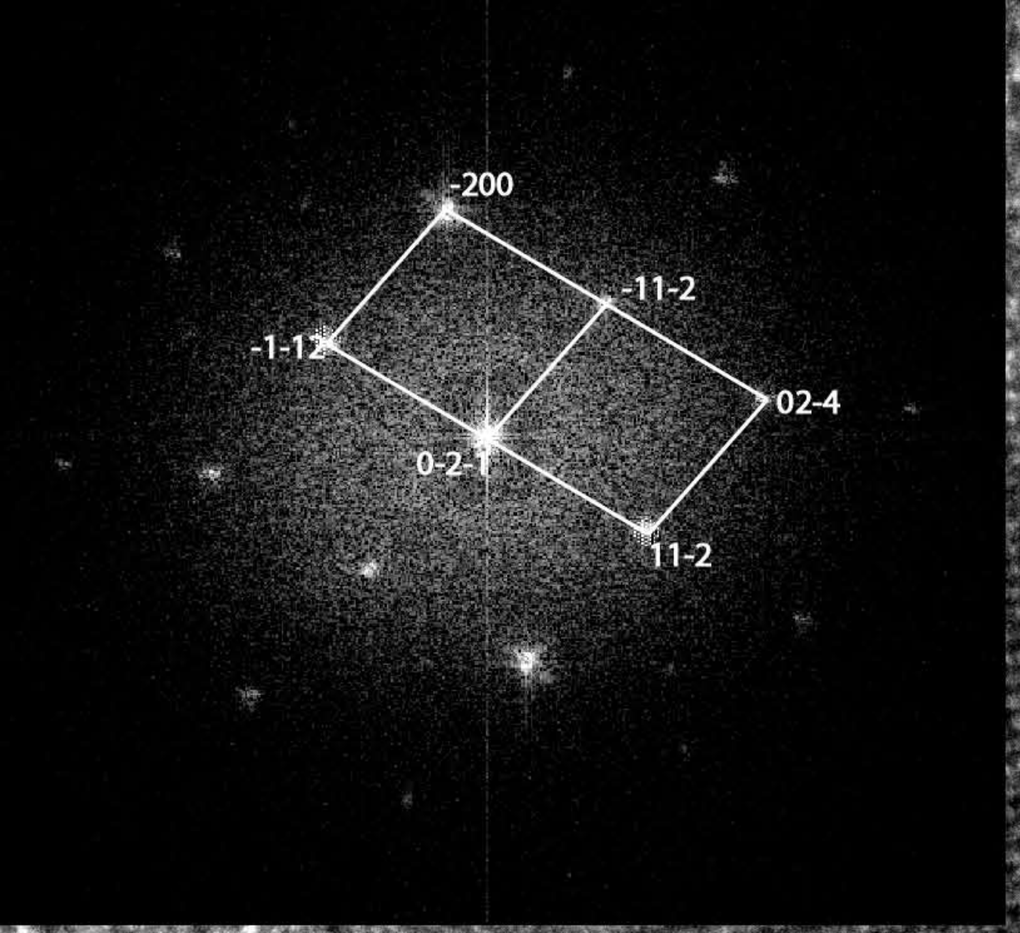
-200
-11-2
-1-12
02-4
0-2-1
11-2

-200
-11-2
11-2
-200
-11-2
5nm

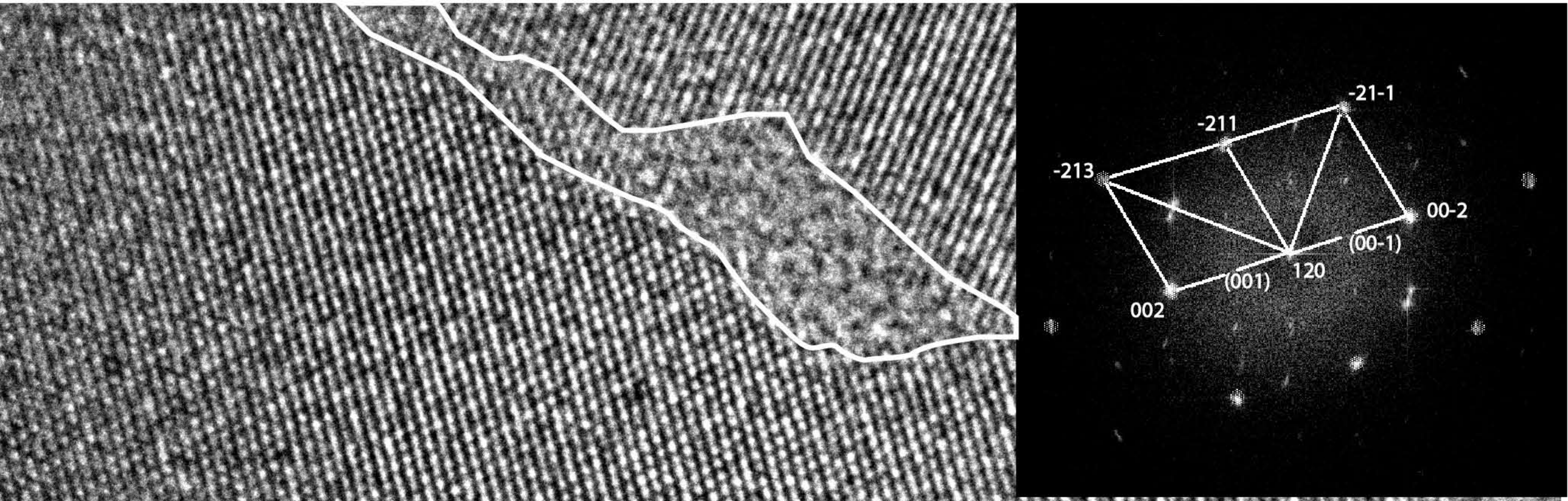
-21-1
-211
-213
00-2
(00-1)
120
(001)
002
5nm

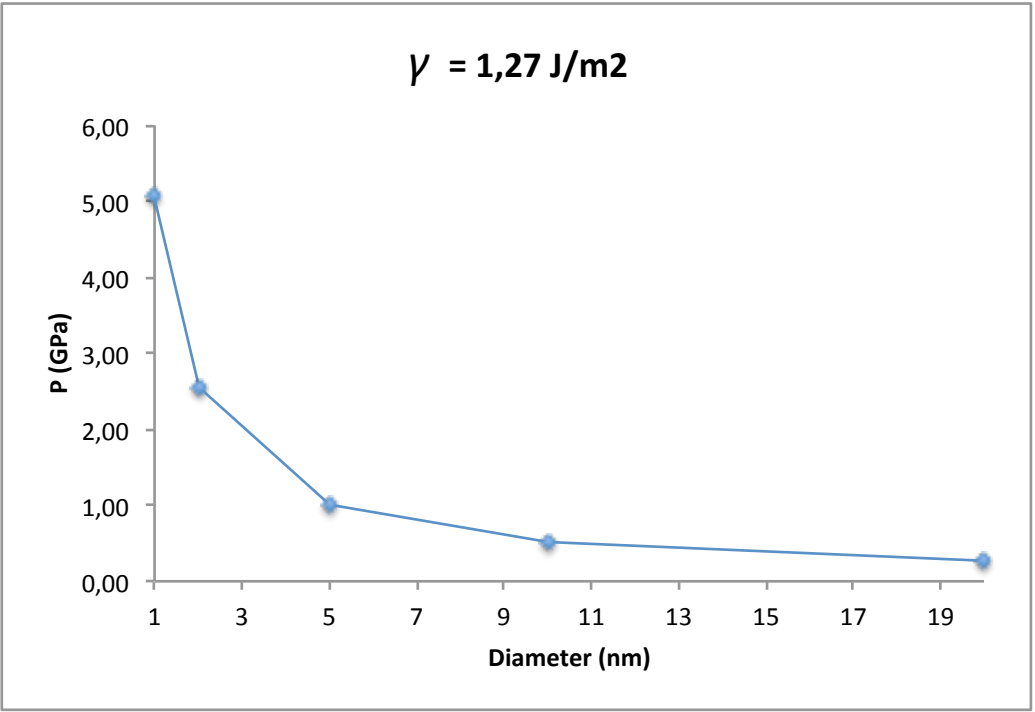
γ = 1,27 J/m2
6,00
5,00
4,00
3,00
2,00
1,00
0,00
P (GPa)
1
3
5
7
9
11
13
15
17
19
Diameter (nm)

b_0= 7,5073 c_0= 12,5160 α = 93,76(2)° β = 98,95(2)° γ = 106,49(2)°		b_0= 6,3715 c_0= 6,3759 α = 93,84(2)° β = 107,34(3)° γ = 107,16(3)°	b_0= 7,9672 c_0= 5,7407	b_0= 4,9760 c_0= 17,4880
3,9150 (-11-2)	6.072	5,9977 (00-1)	3,9836 (020)	3,8654 (01-12)
3,6911 (11-2)	2.994	2,9989 (00-2)	3,7536 (101)	-
2,9611 (-200)	2.961	2,9413 (-211)	-	3,0691 (10-14)
2,4752 (02-4)	2.473	2,3766 (-21-1)	2,4845 (102)	2,4880 (11-20)
	1.867	1,9017 (-213)	1,8607 (013)	1,8923 (11-26)
(02-4)/(11-2) 38,47°	52,94°	(-21-1)/(00-2) 52,03°		
(02-4)/(-11-2) 41,29°	52,20°	(-21-1)/(-211) 50,64°		
(-200)/(-11-2) 52,13°	36,20°	(-213)/(-211) 38,22°		
(-200)/(-1-12) 48,10°	39,08°	(-213)/(002) 39,11°		